BNL-210888-2019-JAAM

The finite size effect on the transport and magnetic properties of epitaxial Fe3O4 thin films

S. Alraddadi, G. Gu

To be published in "MATERIALS EXPRESS"

October 2018

Condensed Matter Physics and Materials Science Department

Brookhaven National Laboratory

U.S. Department of Energy

USDOE Office of Science (SC), Basic Energy Sciences (BES) (SC-22)

DISCLAIMER

The finite size effect on the transport and magnetic properties of epitaxial Fe_3O_4 thin films

Shoroog Alraddadi[1,*], William Hines[2], Genda Gu[3], and Boris Sinkovic[2]
[1]*Department of Physics, Umm Al-Qura University, Makkah 24382, KSA*
[2]*Depatment of Physics, University of Connecticut, Storrs, CT 06269, USA*
[3]*Condensed Matter Physics and Materials Science Department, Brookhaven National Lab, NY 11973, USA*

ABSTRACT
Magnetite (Fe_3O_4) has great potential for use in the new field of spintronics due to its interesting physical properties, e.g., half-metallic ferromagnetic nature and metal–insulator transition (Verwey transition). Therefore, a basic understanding of these properties is essential for applications in spintronics devices, especially as the film thickness is reduced. In this work, the transport and magnetic properties of stoichiometric ultrathin epitaxial Fe_3O_4 films have been investigated. The Fe_3O_4 films were grown on MgO (001) substrates using molecular beam epitaxy under optimal growth conditions. Low energy electron diffraction and X-ray photoemission spectroscopy confirmed that the films are single phase Fe_3O_4. The Verwey transition has been investigated using both transport and magnetization measurements. The magnetization measurements show a sharp Verwey transition in all of these films, which indicates that the films have properties comparable to the bulk. Furthermore, the magnetization measurements at room temperature show that the ultrathin films with thickness t < 20 nm are ferromagnetic with magnetization values greater than those for bulk magnetite. Such enhanced magnetization in ultrathin Fe_3O_4 films is very promising for spin injection and other applications.
Keywords: Epitaxial Growth, Fe_3O_4, Thin Film, Verwey Transition, Magnetization.

1. INTRODUCTION
The studies and applications of magnetite (Fe_3O_4_ thin films have progressed over the last decades due to its unique and interesting electrical and magnetic properties. Fe_3O_4 is an excellent candidate for the realization of spintronics devices[1-3] due to its high Curie temperature (858 K),[4] high spin polarization, and a metalto-insulator transition (Verwey transition) occurring at ≈125 K.[5-6] The epitaxial magnetite thin films have been prepared by different methods on magnesium oxide (MgO) as well as other substrates with various deposition parameters.[7-12] The transport and magnetic properties of Fe_3O_4 have been studied in both bulk and thin films.[6, 11-25] However, the epitaxial thin magnetite films are known to exhibit different magnetic and transport properties from the bulk.[10, 24-26] In particular, increased resistivity with decreasing film thickness,[10, 27-28] broadened Verwey transition,[28, 31-32] superparamagnetism in ultrathin films,[11, 18] decreased saturation magnetization, unusual magnetic anisotropy, and the coercivity field.[33-36] As example at room temperature, the magnetic anisotropy decreases with decreasing Fe_3O_4 thickness and vanishes below 5 nm.[37] These anomalies have been attributed to the film microstructure, stoichiometry, and the presence of structural growth defects called antiphase boundaries APBs.[38-39]
In this work, we have investigated the transport and magnetic properties of stoichiometric epitaxial Fe_3O_4 ultrathin films grown by MBE technique on MgO (001)

substrates. The purpose of this work is to explore the effect of reduced dimension (thickness) and the ordering of Fe^{2+}/Fe^{3+} in ultrathin magnetite on the transport and magnetic properties. Understanding this effect is becoming critical for design and improving the performance of spintronic devices in small size. In order to get films of high-quality, molecular beam epitaxy (MBE) under ultrahigh vacuum was employed. The films were characterized *in-situ* by low energy electron diffraction (LEED) and X-ray photoemission spectroscopy (XPS) as well as *ex-situ* transport and magnetic measurements.

2. EXPERIMENTAL DETAILS

The Fe_3O_4 films were grown by molecular beam epitaxy (MBE) on MgO (001) substrates using a reactive method. This method is ideal for controlling the film thickness and stoichiometry. Molecular beam epitaxy was performed in an ultra-high vacuum chamber with the base pressure lower than $3\_0\times10^{-10}$ torr.

Magnetite thin films of 20 nm, 10 nm, and 5 nm thickness were prepared under optimal growth conditions using reactive MBE as listed in Table I. An optimal and controlled growth process is a crucial requirement for the accurate study of the magnetic and electronic properties of ultrathin Fe_3O_4 films and their application. For this purpose, pure iron rods were thermally evaporated at a deposition rate of 3.33 Å/min with substrate temperatures 250 _C and 265 _C to avoid interdiffusion of magnesium ions from the substrate into the film._[40]_ The details of growth and optimal parameters have been obtained previously._[41]_ The crystal and electronic structures of the films were studied by LEED and XPS (Mg-K__, respectively. Finally, the surfaces of samples were capped with a very thin layer (2 nm) of MgO, in order to avoid transformation to another iron oxide phase.

The resistivity measurements were carried out using closed cycle refrigeration (CCR) system at the University of Connecticut. The magnetization measurements were carried out using a superconducting quantum interference device (SQUID) from Quantum Design at both Brookhaven National Lab and the University of Connecticut.

Table I. The resistivity, saturation magnetization, and temperature of the Verwey transition T_v for (high-quality) Fe_3O_4 films grown on MgO (01) substrates with different thicknesses.

Thickness (nm)	p(O_2) (torr)	Substrate temperature (_C)	Resistivity (_-cm)	T_v (K)	M emu/cm^3 ±30	Hc (Oe)	T_v (K)
20	7×10^{-7}	250	0.0064	122	480	260	121
10	1×10^{-6}	250	0.0516	115	680	160	115
5	7×10^{-7}	265	0.112	No T_v	820	250	100
Bulk	–	–	0.005	125	480	–	124

3. RESULTS AND DISCUSSION

3.1. Structural Properties

The surface crystal structure of the films with different thickness was characterized by LEED. All of the films showed the $(\sqrt{2}\times\sqrt{2})$ $R45$_ surface reconstruction relative to the primitive surface unit cell of magnetite.[42] Figure 1 shows the sharp LEED pattern obtained from a clean MgO (001) substrate and a 5 nm Fe_3O_4 thin film on a MgO (001) substrate, indicating a clean and well-ordered surface structure. Furthermore, the XPS survey spectra over the complete kinetic energy range from 0 to 1253.6 eV of the X-ray (Mg-K_) anode were recorded to check the cleanliness of the surfaces and investigate the composition of the substrates and iron oxide films. All MgO (001) substrates and the iron oxide films were observed to be of good quality and free of contamination.

Fe 2*p* core-level XPS spectra were recorded for Fe_3O_4 films with thicknesses 20 nm, 10 nm, and 5 nm as shown in Figure 2. It is well known that the various iron oxide phases (_-Fe_2O_3, Fe_3O_4, FeO, and Fe) can be distinguished by their characteristic satellite peaks.[8, 40–41] The

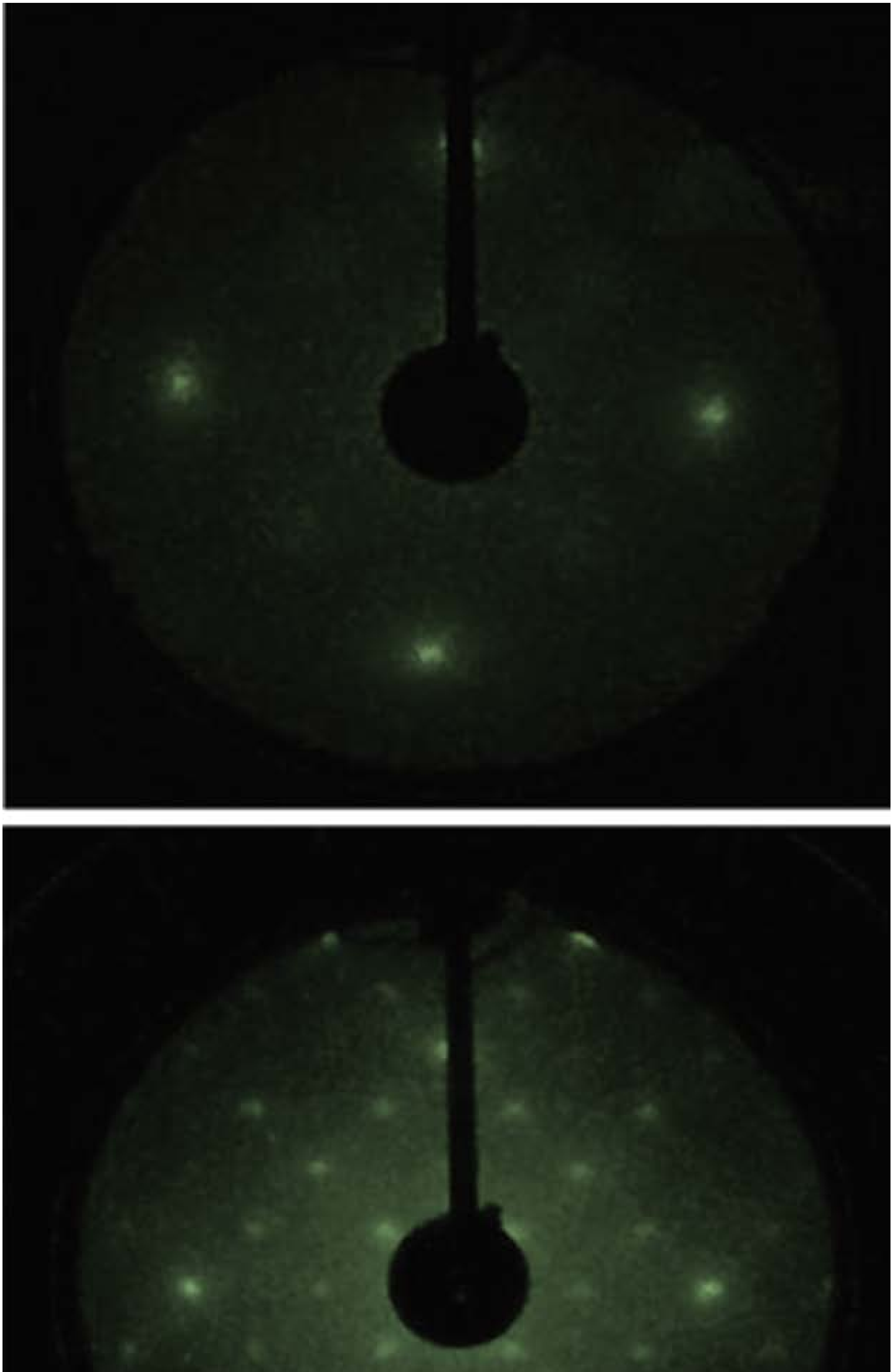

Fig. 1. Low energy electron diffraction pattern with an electron energy of 137 eV for: (a) A clean MgO (001) substrate. (b) An epitaxial 5 nm Fe_3O_4 (001) film grown on an MgO (001) substrate under an oxygen pressure p(O_2_ = 7×10^{-7} torr at a substrate temperature 265 _C.

Fig. 2. Fe 2*p* photoemission spectra obtained with Mg-K_ X-ray radiation for: Epitaxial Fe_3O_4 films with thickness 20 nm, 10 nm, and 5 nm grown on MgO (001) substrates.

Fe 2*p* spectra studied here show no signs of a satellite structure or any metallic Fe clusters, which is taken as an indication of stoichiometric Fe_3O_4. However, the 2*p* peak broadens with decreasing the film thickness, due to the substrate effect, in which some of the XPS charges transfer from the film to the substrate and loose their energy.

3.2. Transport and Magnetic Properties

In order to explore the stoichiometry of the films with reduced thickness, the Verwey transition was investigated using both transport and magnetization measurements. This transition is accompanied by a structural change from a high-temperature cubic phase with the easy magnetization axis along a [100] axis to a low-temperature monoclinic phase with the easy axis aligned along the *c*-axis. The most prominent feature in the electric transport measurements of bulk magnetite is the Verwey transition, observed as a sharp change in resistivity occurring at 120 K, which is attributed to a charge ordering at the octahedral sites. The temperature dependence of the resistivity for the films grown with various thicknesses is shown in Figure 3.

As the thickness of the Fe_3O_4 films is reduced, the Verwey transition broadens and vanishes for the 5 nm film, which is indicative of the breaking of long range charge ordering associated with this transition. Furthermore, it is observed that the Fe_3O_4 film resistivity increases with decreasing thickness. It was reported that the impact on scattering due to imperfections in the vicinity of the surface and interface with the substrate will be larger for the thinner films relative to the thicker ones._10_ 36_ Thus, it is to be expected that the thinner films will have higher resistivity. The higher resistivity values for the Fe_3O_4 films with thickness <20 nm compared to the bulk, the reduction of T_v, and the broadening of the Verwey

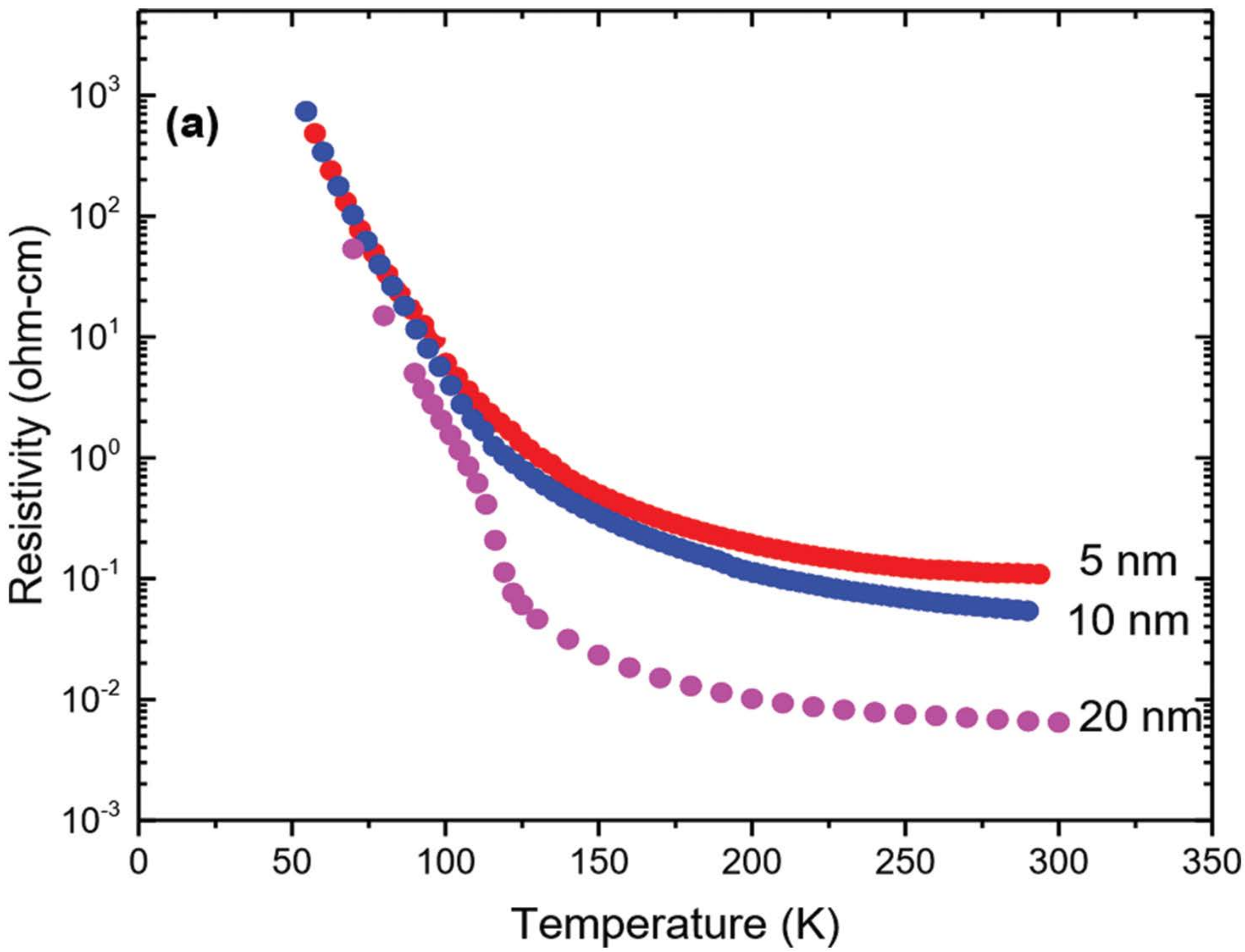

(a)
Resistivity (ohm-cm)
Temperature (K)
5 nm
10 nm
20 nm
10^3
10^2
10^1
10^0
10^{-1}
10^{-2}
10^{-3}
0
50
100
150
200
250
300
350

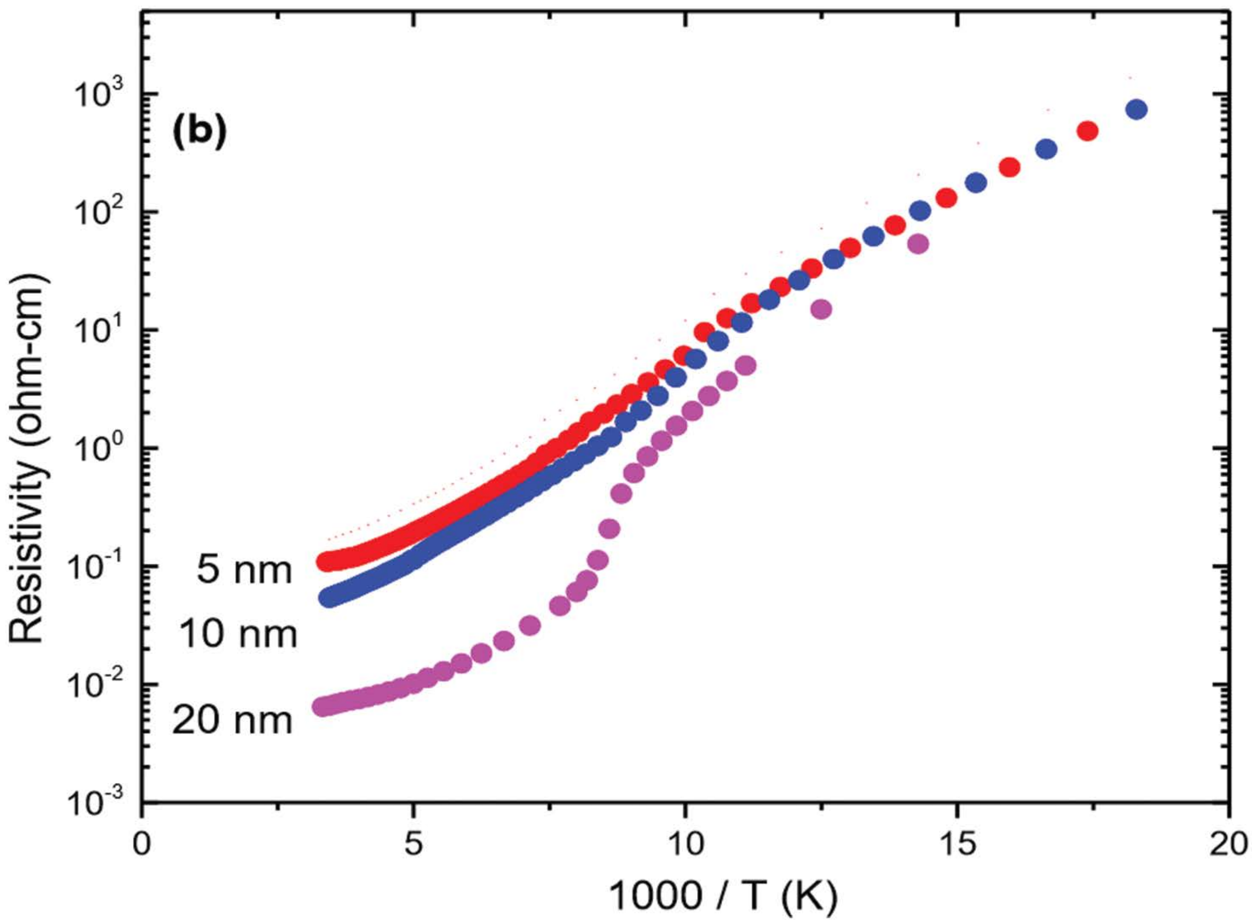

Fig. 3. (a) Semilog plot of resistivity (ohm-cm) versus temperature (K) during warming of the 20 nm, 10 nm, and 5 nm Fe_3O_4 films grown on MgO (001) substrates. (b) Semilog plot of resistivity (ohm-cm) versus 1000/temperature (1/K) during warming for the same Fe_3O_4 films.

transition may be attributed to increase the antiphase boundaries (APBs) density, thus a significant decrease in domain size.[10, 11, 38, 45] It was reported that the increase of the resistivity with decreasing film thickness and the absence of the Verwey transition in films thinner than 25 nm may be also related to very small structural domain size.[10] In contrast, a recent study still observed a clear Verwey transition in 10 nm thick film.[46]

In conclusion, it seems that determination of the Verwey transition by transport measurements is difficult in ultrathin films, due to the film discontinuity, the decreased domain size, and the presence of the surface and/or interface with the substrate.[47] Therefore, since the magnetic measurements are less affected by the domain size, in the next section we will focus on magnetization studies of the effect of the reduced thickness on the properties of ultrathin

films.
The temperature dependence of the zero fieldcooled
(ZFC) and field-cooled (FC) magnetization curves

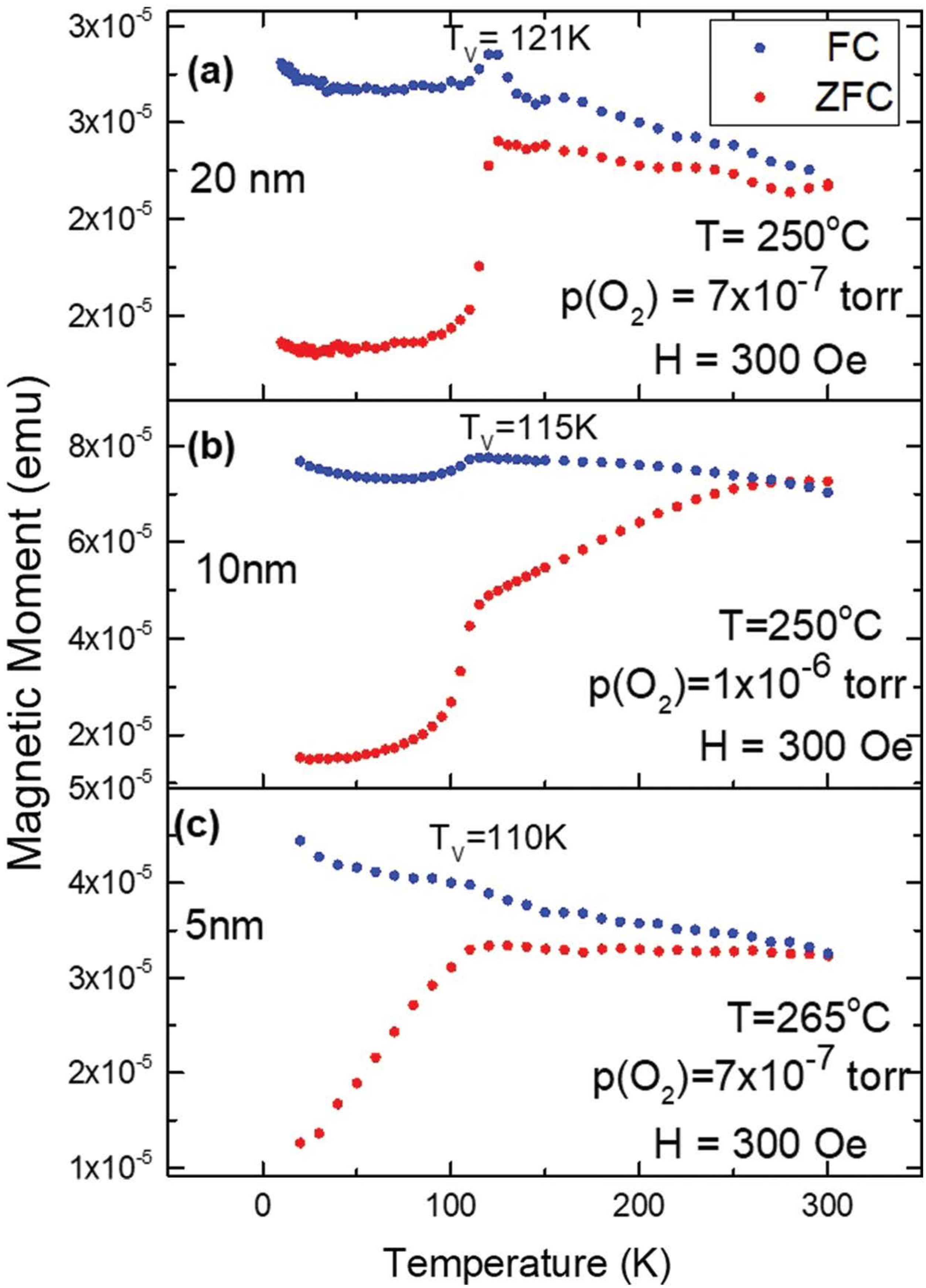

Magnetic Moment (emu)
Temperature (K)
FC
ZFC
(a)
T_V= 121K
20 nm
T= 250°C
p(O_2) = 7x10^-7 torr
H = 300 Oe
(b)
T_V=115K
10nm
T=250°C
p(O_2)=1x10^-6 torr
H = 300 Oe
(c)
T_V=110K
5nm
T=265°C
p(O_2)=7x10^-7 torr
H = 300 Oe

Fig. 4. Total magnetic moment (emu) versus temperature (K) during heating (red circles), and subsequent cooling (blue circles), for Fe_3O_4 films grown on MgO (001) substrates with various thicknesses (a) 20 nm, (b) 10 nm, and (c) 5 nm, oxygen pressure and substrate temperature values are indicated.

measured for different film thicknesses are shown in Figure 4. The measurements were made with a magnetic field of 300 Oe applied in the (001) plane of the film. A sharp Verwey transition was found in all of the films. The first derivative of ZFC curve for the 20 nm, 10 nm, and 5 nm films suggests that the Verwey transition occurs at about 121 K, 115 K, and 110 K, respectively. Figure 5

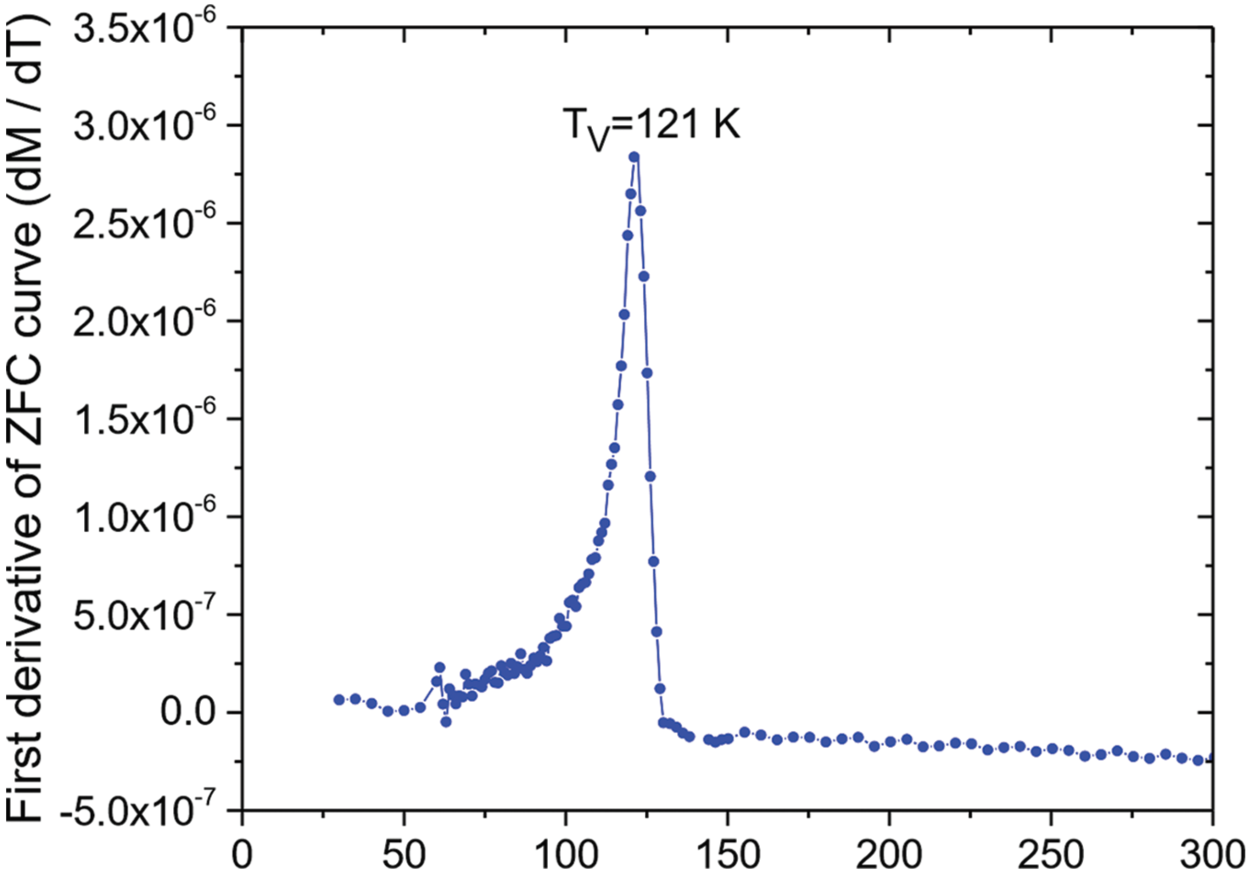

Fig. 5. Temperature derivative of the data of Figure 3(a) for 20 nm Fe_3O_4 film grown on a MgO (001) substrate under oxygen pressure 7×10^{-7} torr.

shows the first derivative of the ZFC curve for the 20 nm film grown with $p(O_2)$ = 7_0$\times10^{-7}$ torr.
Magnetic hysteresis loops for the Fe_3O_4 films were measured at 300 K by applying the magnetic field in the (001) plane of the film. All of these films exhibit ferromagnetic behavior. Figure 6(a) shows the total magnetic moment for the three samples with different film thickness

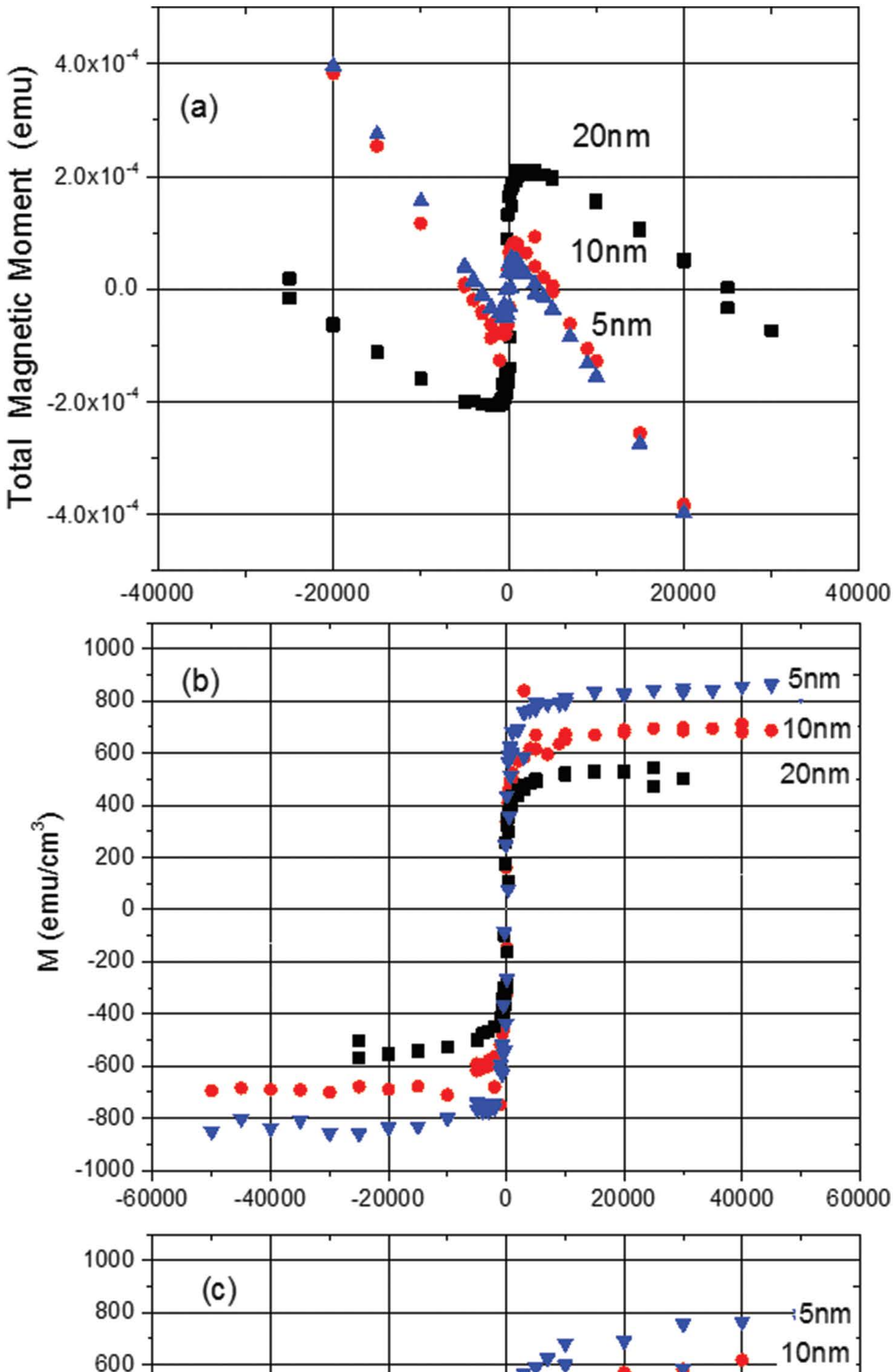

Total Magnetic Moment (emu)
4.0x10-4
2.0x10-4
0.0
-2.0x10-4
-4.0x10-4
(a)
20nm
10nm
5nm
-40000
-20000
0
20000
40000
M (emu/cm3)
1000
800
600
400
200
0
-200
-400
-600
-800
-1000
(b)
5nm
10nm
20nm
-60000
-40000
-20000
0
20000
40000
60000
1000
800
600
(c)
5nm
10nm

Fig. 6. (a) Total magnetic moment (emu) versus magnetic field (Oe), hysteresis loops, obtained at 300 K for the 20 nm,10 nm, and 5 nm films grown on MgO (001) substrates. (b) Film magnetization (emu/cm3_, obtained from the data in (a) corrected for the MgO substrate contribution. (c) The magnetic field behavior around the origin for the films.

while Figures 6(b) and (c) show the film magnetization and coercivity. The small coercivity (Hc) observed in our films is representative of a weak pinning of the magnetic domains.[47] The magnetization of 20 nm, 10 nm, and 5 nm films were found to be 480 emu/cm^3, 680 emu/cm^3, and 820 emu/cm^3, respectively. The 10 nm, and 5 nm Fe_3O_4 films have enhanced magnetization compared to the bulk value, which might be promising for the spintronics applications such as spin injunction into semiconductors. This result is in contradiction with some earlier studies that suggest a dead interface layer or a superparamagnetic behavior for ultrathin films of magnetite caused by the APBs. Voogt et al.[28] and Eerenstein et al.[31] showed that the ultrathin Fe_3O_4 films are superparamagnetic. Table I summarizes the transport and magnetic properties for high-quality Fe_3O_4 films grown on MgO (001) substrates with different thicknesses.

It has been suggested that the enhancement of the magnetization for Fe_3O_4 films ≤10 nm is due to the presence of APBs defects which contribute to the unusual magnetic properties of Fe_3O_4 thin films, such as broadening of the Verwey transition, and the non-saturation of magnetization, even at a very high magnetic field.[28, 48–50] This interesting phenomenon was observed recently in Fe_3O_4 films.[50, 51] However, the origin of such high magnetization is still under debate. On the one hand, it was suggested that APBs and the uncompensation of spin moments at the surface are main factors contributing to the observed enhanced magnetic moment.[47] On the other hand, it was attributed to the presence of Fe impurities in the substrate that enhanced the magnetization.[51] In the very recent study,[52] it was revealed by using that the magnetization enhancement is due to spin-flipping of valence spins in tetrahedral-Fe^{3+} at Fe_3O_4 grain boundaries via oxygen, enhancing the overall double-exchange and suppressing the super-exchange interactions. From these previous studies, it is clear that the magnetization property of magnetite thin film strongly depends on the method of preparation, nature of defects and the defect density.

It is imperative to recognize whether or not our observation of such a large magnetization for the thinner (<20 nm) magnetite films is real or not. The first possibility for error is related to the film thickness. This is ruled out due to the fact that the growth rate and the thickness values of the films are accurately measured (90–95%) using XPS. The second possibility is the contribution of impurities in the MgO substrate, which has been corrected for yielding a signal that is attributed to the film itself. Magnetization measurements on a MgO substrate treated and annealed in the same environment as those used for the growth of the Fe_3O_4 films showed an absence of any magnetic contamination at room temperature and low temperatures. Furthermore, the possibility of a non-stoichiometric phase or any Fe clustering is also ruled out. No evidence

for the presence of any other iron oxide phase or unreacted Fe was found from LEED and XPS studies. Moreover, the transformation of magnetite to the Fe_2O_3 or FeO phase would lead to a reduction in the magnetization as both of these phases have a smaller magnetization than the Fe_3O_4 phase. In addition to structural investigations, we also investigated the stoichiometry of these films using the Verwey transition through magnetic measurements as shown in Figure 4. The growth temperature is low and, therefore, the possibility of Mg interdiffusion into the films_53_ is also ruled out. Furthermore, the tendency of Mg^{+2} ions to substitute at octahedral (B)-sites, will lead a reduction in the magnetic moment rather than enhancing it.

4. CONCLUSION

In summary, high quality epitaxial Fe_3O_4 ultrathin films ($\leq$20 nm) were grown on MgO (001) substrates using a reactive MBE under the optimal conditions for each thickness. In this work, the effect of reduced thickness on the transport and magnetic properties of high quality epitaxial Fe_3O_4 ultrathin films has been investigated. By characterizing the films structurally, a complete picture of epitaxial Fe_3O_4 ultrathin films was obtained. Since the magnetic and transport properties of Fe_3O_4 are strongly correlated with quality of crystal structure.

The resistivity of ultrathin Fe_3O_4 films with thickness <20 nm showed very high value compared to the bulk, with a broadening of the Verwey transition; and the transition vanishes in the 5 nm film. However, the magnetization measurement showed a sharp Verwey transition in all of the films. Furthermore, the ultrathin Fe_3O_4 films displayed a ferromagnetic behavior with saturation magnetization values that are much greater than that of bulk magnetite, particularly for thicknesses <20 nm. This observation of an enhanced magnetization in ultrathin magnetite film is very promising for the spintronics application such as spin injection.

Acknowledgments: The authors would like to acknowledge the support of the Physics Department at the University of Connecticut.

References and Notes

1. I. Žuti´c, J. Fabian, and S. D. Sarma; Spintronics: Fundamentals and applications; *Rev. Mod. Phys.* 76, 323 (2004).
2. M. Ziese; Extrinsic magnetotransport phenomena in ferromagnetic oxides; *Rep. Prog. Phys.* 65, 143 (2002).
3. J. M. D. Coey and M. Venkatesan; Half-metallic ferromagnetism: Example of CrO_2; *J. Appl. Phys.*, 91, 8345 (2002).
4. M. L. Glasser and F. J. Milford; Spin wave spectra of magnetite; *Phys. Rev.* 130, 1783 (1963).
5. F. Walz; The Verwey transition-a topical review; *J. Phys. Condens.*

Matter 14, R285 (2002).
6. E. J. W. Verwey; Electronic conduction of magnetite (Fe_3O_4) and its transition point at low temperatures; *Nature* 144, 327(1939).

7. J. Korecki, B. Handke, N. Spiridis, T. ´ Sl¸ezak, F. Flis-Kabulska, and J. Haber; Size effects in epitaxial films of magnetite; *Thin Solid Films* 412, 14 (2002).
8. Y. Gao and S. A. Chambers; Heteroepitaxial growth of _-Fe_2O_3, _-Fe_2O_3 and Fe_3O_4 thin films by oxygen-plasma-assisted molecular beam epitaxy; *J. Cryst. Growth* 174, 446 (1997).
9. S. A. Chambers and S. A. Joyce; Surface termination, composition and reconstruction of Fe_3O_4 (001) and _-Fe_2O_3 (001); *Surf. Sci.* 420, 111 (1999).
10. W. Eerenstein, T. T. M. Palstra, T. Hibma, and S. Celotto; Origin of the increased resistivity in epitaxial Fe_3O_4 films; *Phys. Rev. B* 66, 201101 (2002).
11. X. Liu, C. F. Chang, A. D. Rata, A. C. Komarek, and L. H. Tjeng; Fe_3O_4 thin films: Controlling and manipulating an elusive quantum material; *npj Quantum Materials* 1, 16027 (2016).
12. X. Wang, Y. Liao, D. Zhang, T. Wen, and Z. Zhong; A review of Fe_3O_4 thin films: Synthesis, modification and applications; *J. Mater. Sci. Technol.* 34, 1259 (2018).
13. S. K. Arora, R. G. S. Sofin, I. V. Shvets, R. Kumar, M. W. Khan, and J. P. Srivastava; Influence of antiphase boundary density on the conduction noise properties of epitaxial magnetite thin films; *J. Appl. Phys.* 97, 10C310 (2005).
14. R. Ramos, S. K. Arora, and I. V. Shvets; Influence of miscut on the anisotropic magnetoresistance of magnetite thin films; *J. Appl. Phys.* 105, 07B108 (2009).
15. J. Yoshida and S. Iida; X-ray diffraction study on the low temperature phase of magnetite; *J. Phys. Soc. Jap.* 42, 230 (1977).
16. R. Ramos, S. K. Arora, and I. V. Shvets; Anomalous anisotropic magnetoresistance in epitaxial Fe_3O_4 thin films on MgO (001); *Phys. Rev. B* 78, 214402 (2008).
17. S. P. Sena, R. A. Lindley, H. J. Blythe, C. Sauer, M. Al-Kafarji, and G. A. Gehring; Investigation of magnetite thin films produced by pulsed laser deposition; *J. Magn. Mag. Mater.* 176, 111 (1997).
18. M. Ziese and H. J. Blythe; Magnetoresistance of magnetite; *J. Phys.: Condens. Matter* 12, 13 (2000).
19. M. G. Chapline and S. X. Wang; Observation of the Verwey transition in thin magnetite films; *J. Appl. Phys.* 97, 123901 (2005).
20. Y. Zhou, C. McEvoy, R. Ramos, and I. V. Shvets; The magnetic and magnetoresistance properties of ultrathin magnetite films grown on MgO substrate; *J. Appl. Phys.* 99, 08J111 (2006).
21. X. W. Li, A. Gupta, G. Xiao, and G. Q. Gong; Transport and magnetic properties or epitaxial and polycrystalline magnetite thin films; *J. Appl. Phys.* 83, 7049 (1998).
22. N. F. Mott; Metal-Insulator Transitions, 2nd edn., Taylor and Francis, London (1990), p. 215.
23. J. García, G. Subías, M. G. Proietti, J. Blasco, H. Renevier, J. L. Hodeau, and Y. Joly; Absence of charge ordering below the Verwey transition temperature in magnetite; *Phys. Rev. B* 63, 054110 (2001).
24. W. Kündig and R. S. Hargrove; Electron hopping in magnetite; *Solid State Commun.* 7, 223 (1969).
25. R. Aragón, D. J. Buttrey, J. P. Shepherd, and J. M. Honig; Influence of nonstoichiometry on the Verwey transition; *Phys. Rev. B* 31, 430 (1985).
26. D. T. Marailies, F. T. Parker, M. L. Rudee, F. E. Spada, J. N. Chapman, P. R. Aitchison, and A. E. Berkowitz; Origin of the anomalous magnetic behavior in single crystal Fe_3O_4 films; *Phys. Rev. Lett.* 79, 5162 (1997).
27. W. Ecrenstein, T. T. M. Palstra, S. S. Saxena, and T. Hibma; Spinpolarized transport across sharp antiferromagnetic boundaries; *Phys. Rev. lett.* 88, 247204 (2002).
28. F. C. Voogt, T. T. Palstra, L. Niesen, O. C. Rogojanu, M. A. James, and T. Hibma; Superparamalmetic behavior of structural domains in epitaxial ultrathin magnetite films; *Phys. Rev. B* 57, 88107 (1998).

29. A. V. Ramos, J. B. Moussy, M. J. Guittet, A. M. Bataille,
M. Gautier-Soyer, M. Viret, C. Gatel, and E. Snoeck; Magnetotransport properties of Fe_3O_4 epitaxial thin films: Thickness effects driven by antiphase boundaries; *J. Appl. Phys.* 100, 103902 (2006).
30. X. W. Li, A. Gupta, G. Xiao, and G. Q. Gong; Transport and magnetic properties of epitaxial and polycrystalline magnetite thin films; *J. Appl. Phys.* 83, 7049 (1998).
31. W. Eerenstein, T. Hibma, and S. Celotto; Mechanism for superparamagnetic behavior in epitaxial Fe_3O_4 films; *Phys. Rev. B* 70, 184404 (2004).
32. R. G. S. Sofin, S. K. Arora and I. V. Shvets; Study of magnetoresistance of epitaxial magnetite flints grown on vicinal MgO (100) substrate; *J. Appl. Phys.* 97, 100315 (2005).
33. C. Cheng; Structure and magnetic properties of the Fe_3O_4 (001) surface: *Ab initio* studies; *Phys. Rev. B* 71, 052401 (2005).
34. Y. Zhou, X. Jin, and I. V. Shvets; Enhancement of the magnetization saturation in magnetite (100) epitaxial films by thermo-chemical treatment; *J. Appl. Phys.* 95, 7357 (2004).
35. S. K. Arora, R. G. S. Sofin, I. V. Shvets, and M. Luysberg; Anomalous strain relaxation behavior of Fe_3O_4/MgO (100) heteroepitaxial system grown using molecular beam epitaxy; *J. Appl. Phys.* 100, 073908 (2006).
36. J. Korecki, B. Handke, N. Spurudis, T. Slezak, I. Flis-Kabulska, and J. Haber; Size effects in epitaxial films of magnetite; *Thin Solid Films* 412, 14 (2002).
37. P. A. A. Van der Heijden, M. G. Van Opstal, C. H. W. Swüste, P. H. J. Bloemen, J. M. Gaines, and W. J. M. De Jonge; A ferromagnetic resonance study on ultra-thin Fe_3O_4 layers grown on (001) MgO; *J. Magn. Magn. Mater.* 182, 71 (1998).
38. D. T. Margulies, F. T. Parker, F. E. Spada, R. S. Goldman, J. Li, R. Sinclair, and A. E. Berkowitz; Origin of the anomalous magnetic behavior in single crystal Fe_3O_4 films; *Phys. Rev. Lett.* 79, 5162 (1997).
39. D. T. Margulies, F. T. Parker, F. E. Spada, R. S. Goldman, J. Li, R. Sinclair, and A. E. Berkowitz; Anomalous moment and anisotropy behavior in Fe_3O_4 films; *Phys. Rev. B* 53, 9175 (1996).
40. Y. Gao, Y. J. Kim, and S. A. Chambers; Preparation and characterization of epitaxial iron oxide films; *J. Mater. Res.* 13, 2003 (1998).
41. S. Alraddadi, W. Hines, T. Yilmaz, G. D. Gu, and B. Sinkovic; Structural phase diagram for ultra-thin epitaxial Fe_3O_4 /MgO (001) films: Thickness and oxygen pressure dependence; *J. Phys.: Condens. Matter* 28, 115402 (2016).
42. F. Y. Ran, Y. Tsunemaru, T. Hasegawa, Y. Takeichi, A. Harasawa, K. Yaji, S. Kim, and A. Kakizaki; Angle-resolved photoemission study of Fe_3O_4 (001) films across Verwey transition; *J. Phys. D: Appl. Phys.* 45, 275002 (2012).
43. Y. Gao, Y. J. Kim, S. A. Chambers, and G. Bai; Synthesis of epitaxial films of Fe_3O_4 and _-Fe_2O_3 with various low-index orientations by oxygen-plasma-assisted molecular beam epitaxy; *J. Vac. Sci. Technol., A: Vacuum. Surfaces, and Films* 15, 332 (1997).
44. Y. Gao, Y. J. Kim, S. A. Chambers, and G. Bai; *In situ* XPS analysis of various iron oxide films grown by NO_2-assisted molecular-beam epitaxy; *Phys. Rev. B* 59, 3195 (1999).
45. T. Kado; Structural and magnetic properties of magnetite-containing epitaxial iron oxide films grown on MgO (001) substrates; *J. Appl. Phys.* 103, 043902 (2008).
46. X. H. Liu, A. D. Rata, C. F. Chang, A. C. Komarek, and L. H. Tjeng; Verwey transition in Fe_3O_4 thin films: Influence of oxygen stoichiometry and substrate-induced microstructure; *Phys. Rev. B* 90, 125142 (2014).
47. S. K. Arora, H. C. Wu, R. J. Choudhary, I. V. Shvets, O. N. Mryasov, H. Z. Yao, and W. Y. Ching; Giant magnetic moment in epitaxial Fe_3O_4 thin films on MgO (100); *Phys. Rev. B* 77, 134443 (2008).

48. D. Zhang, Z. Liu, S. Han, C. Li, B. Lei, M. P. Stewart, J. M. Tour, and C. Zhou; Magnetite (Fe_3O_4) core–shell nanowires: Synthesis and

magnetoresistance; *Nano Lett.* 4, 2151 (2004).
49. R. G. S. Sofin, S. K. Arora, and I. V. Shvets; Positive antiphase boundary domain wall magnetoresistance in Fe_3O_4 (110) heteroepitaxial films; *Phys. Rev. B* 83, 134436 (2011).
50. W. Eerenstein, T. Palstra, T. Hibma, and S. Celotto; Diffusive motion of antiphase domain boundaries in Fe_3O_4 films; *Phys. Rev. B* 68, 014428 (2003).
51. J. Orna, P. A. Algarabcl, L. Morellón, J. A. Pardo, J. M. de Teresa, R. L. Antón, F. Bartolomé, L. M. García, J. Bartolomé, J. C. Cezar, and A. Wildes; Origin of the giant magnetic moment in epitaxial Fe_3O_4 thin films; *Phys. Rev. B* 81, 144420 (2010).
52. T. S. Herng, W. Xiao, S. M. Poh, F. He, R. Sutarto, X. Zhu, R. Li, X. Yin, C. Diao, Y. Yang, X. Huang, X. Yu, Y. Ping Feng, A. Rusydi, and J. Ding; Achieving a high magnetization in sub-nanostructured magnetite films by spin-flipping of tetrahedral Fe^{3+} cations; *Nano Res.* 8, 2935 (2015).
53. K. A. Shaw, E. Lochner, and D. M. Lind; Interdiffusion study of magnesium in magnetite thin films grown on magnesium oxide (001) substrates; *J. Appl. Phys.* 87, 1727 (2000).